Cell Cycle

ISSN: 1538-4101 (Print) 1551-4005 (Online) Journal homepage: http://www.tandfonline.com/loi/kccy20

Modulation of the p53-MDM2 Interaction by Phosphorylation of Thr18: A Computational Study

Hui Jun Lee, Deepa Srinivasan, David Coomber, David P. Lane & Chandra S. Verma

To cite this article: Hui Jun Lee, Deepa Srinivasan, David Coomber, David P. Lane & Chandra S. Verma (2007) Modulation of the p53-MDM2 Interaction by Phosphorylation of Thr18: A Computational Study, Cell Cycle, 6:21, 2604-2611, DOI: 10.4161/cc.6.21.4923

To link to this article: https://doi.org/10.4161/cc.6.21.4923

Published online: 08 Nov 2007.

[Cell Cycle 6:21, 2604-2611, 1 November 2007]; ©2007 Landes Bioscience

Extra View

Modulation of the p53-MDM2 Interaction by Phosphorylation of Thr18

A Computational Study

Hui Jun Lee[1]
Deepa Srinivasan[2]
David Coomber[2]
David P. Lane[2]
Chandra S. Verma[1,*]

[1]Bioinformatics Institute; Singapore

[2]Institute of Molecular and Cell Biology; Singapore

*Correspondence to: Chandra Verma; Bioinformatics Institute; 30 Biopolis Street; #07-01 Matrix; Singapore 138671; Phone: 65.64788273; Fax: 65.64789048 Email: chandra@bii.a-star.edu.sg

Original manuscript submitted: 08/18/07
Manuscript accepted: 08/20/07

Previously published online as a *Cell Cycle* E-publication: http://www.landesbioscience.com/journals/cc/article/4923

KEY WORDS

p53, p53TAD, MDM2, MDM4, phosphorylations, electrostatics, helicity

ABBREVIATIONS

MDM2	murine double minute clone 2
p53TAD	p53 transactivation domain
hbond	hydrogen bond

ACKNOWLEDGEMENTS

This work has been supported by A*STAR (Agency of Science, Technology and Research). BII and IMCB are A*STAR research institutes. We thank the editor for bringing to our attention some crucial references.

NOTE

Supplemental materials can be found at: http://www.bii.a-star.edu.sg/~chandra/HJ-cellcyclep53phos-suppfigs.pdf

ABSTRACT

The transcription factor p53 is under negative regulation by the ubiquitin ligase MDM2 and its close homologue MDM4. In the bound complex between MDM2 and p53, the transactivation domain of p53 adopts an amphipathic helical conformation which optimizes the spatial organization of three key hydrophobic residues (Phe19, Trp23, Leu26) for maximum interactions. The interaction with MDM2 is known to be abrogated by phosphorylation of Ser/Thr residues in the MDM2 N-terminal domain and in the p53 transactivation domain. In the latter, phosphorylation of Thr18 has been attributed to destabilize a key hbond between Thr18 and Asp21. This interaction has been thought to be critical for the formation of the helical conformation of the p53 transactivation domain. Molecular dynamics simulations of the p53 transactivation domain suggest that phosphorylation of either Thr18 or Ser20 does not disrupt its helical structure but does result in reduced affinities for MDM2. While interactions between the Thr18 and Asp21 are indeed broken due to charge-charge repulsions, the peptide has enough inherent flexibility to form alternate patterns of hbonds, resulting in the maintenance of helicity. Electrostatics of MDM2 reveal local anionic patches in the region where Thr18 docks. These suggest that repulsions will arise because the MDM2 surface will force the p53 to bind in a manner that will place the negatively charged phosphorylated Thr18 near this anionic region. A similar, albeit somewhat attenuated pattern of electrostatic modulations, is seen for a model of MDM4 that has been built. Mutants of MDM2 and MDM4 have been designed to attenuate this anionicity and have been computationally demonstrated to enhance the binding of the phosphorylated peptides.

INTRODUCTION

p53 is a tumor suppressor transcription factor, known to be implicated in more than 50% of all human cancers.[1] Under normal conditions, p53 is quiescent and present at basal levels. Upon cellular stress, DNA damage and hypoxia, it is upregulated and induces pathways that cause cell cycle arrest, DNA repair, cellular senescence, differentiation and apoptosis.[2,3] Due to its ability in arresting cell growth, p53 activity is tightly regulated under non-stressed conditions.[4,5] Under stress, in order to ensure rapid activation of p53, its activity[6] is regulated through control of its stability, sub-cellular localization and post-translational modifications.

The stability of p53 is largely controlled by the oncoprotein murine double minute clone 2 (MDM2, HDM2).[7] This is an E3 ubiquitin ligase and is known to bind to p53 and lead to its proteasomal degradation. Simultaneously, MDM2 is also a downstream target of p53; this creates a negative feedback loop with p53 activating MDM2, which in turn, downregulates p53.[8,9] Under normal conditions, p53 is in equilibrium between being synthesized and degraded by MDM2. However, some p53 escapes thereby enabling the maintenance of the feedback loop by transcribing the MDM2 gene; this leads to normal cell proliferation. When the cell receives a stress signal, chemical modifications of p53 and MDM2 occur as a result of which the binding of MDM2 to p53 is blocked or altered, disrupting the proteolysis of p53. The accumulation of p53 in the cell then leads to upregulation of the various p53-dependent genes.[7] This also includes the transcription of MDM2, but the MDM2 gene product fails to interact properly with p53 due to modifications on both partners and hence does not affect p53 levels. If the cellular damage is repaired then there are no more protein modifications leading to the reformation of the p53-MDM2 complex. Thereafter, the amount of p53 will again be brought to a basal level and the transactivation of p53-responsive genes would cease. The cells resume normal

progression through the cell cycle. In cases where the damage is too great to revive the cell, the p53 activated death pathway will lead to apoptosis. More recently the protein MDM4 (MDMX, HDM4, HDMX) which was discovered about a decade ago[10] has been found to play an increasingly intimate role in the biology p53[11] both by directly interacting with p53 and with MDM2, largely by destabilizing increased MDM2 levels under stressful conditions.[12,13] While MDM2 has long been recognized as therapeutically important, it is now becoming increasingly apparent that MDMX is also a potential target for tumours expressing wild type p53.[11]

Structural and biochemical characterization of the p53-MDM2 complex reveals that they are held together largely by hydrophobic interactions[14] involving the N-terminal domain of MDM2 and the N-terminal transactivation domain of p53 (p53TAD) and separately, the central domain of MDM2.[15] The crystal structure (Protein Data Bank entry 1YCR, resolved at 2.6Å[14]) of the N-terminus of MDM2 (residues 25–109) bound to a fragment of the p53TAD (residues 17–29) shows a deep hydrophobic groove of MDM2 accommodating residues on the non-polar side of an amphipathic helical p53 peptide (Fig. 1A). The hydrophobic core of MDM2 consists of 14 conserved hydrophobic and aromatic residues (Fig. S1A; henceforth the numbering of figures and tables that are given as supplementary information will be prefixed with the letter S) from three different secondary structural elements.[14] They are Met50, Leu54, Leu57, Gly58, Ile61 and Met62 from the α2-helix, Tyr67, His73, Val75, Phe91 and Val93 from the β-sheet and His96, Ile99 and Tyr100 from the α2'-helix. These residues make extensive van der Waals contacts with p53, specifically with Phe19, Trp23 and Leu26 (Fig. 1B). These three residues are highly conserved (Fig. S1B) and are believed to be implicated in transactivation.[16,17] This suggests that MDM2 inhibits p53 activity by concealing its transactivation domain and prevents target genes from being activated. MDM2 and MDM4 show the highest level of sequence similarity in their N-terminal regions and it is this region that binds the transactivation domain of p53 (Fig. S1A). The residues of MDM2 that are involved in making contacts with p53 are mostly conserved in MDM4. Peptides derived from the transactivation segment of p53 have been demonstrated to bind to both MDM2 and MDM4, albeit with reduced affinity in the latter.[18] A structural study of a "humanized" zebrafish MDM4 where the p53-binding site residues of zebrafish MDM4 have been mutated to those of the human form has been reported.[19] Their main findings were that a part of the p53-binding cleft is altered in its conformation compared to that seen in the structure of MDM2.

Phosphorylation of Ser/Thr residues is one of the major post-translational modifications that modulate interactions of p53 with other proteins and is carried out by several kinases.[20-24] UV or IR exposure causes DNA damage that activates ATM (ataxia telangiectasia mutated) and ATR (ATM and Rad3 related). These in turn phosphorylate Chk1 (Checkpoint kinases 1), Chk2 and p53.[21,25] In response to DNA damage, Ser15 of p53 is immediately phosphorylated[26] but has little effect in disrupting the p53-MDM2 association.[27] Substitution of Ser15 with alanine has little effect on the ubiquitination and degradation of human p53 but does enhance the interaction of p53 with transcriptional coactivators p300/CBP.[28] In contrast, p53 phosphorylation sites that are within the p53-MDM2 interaction domain, i.e., Thr18 and Ser20, are known to interfere with complexation upon phosphorylations.[29] Both these

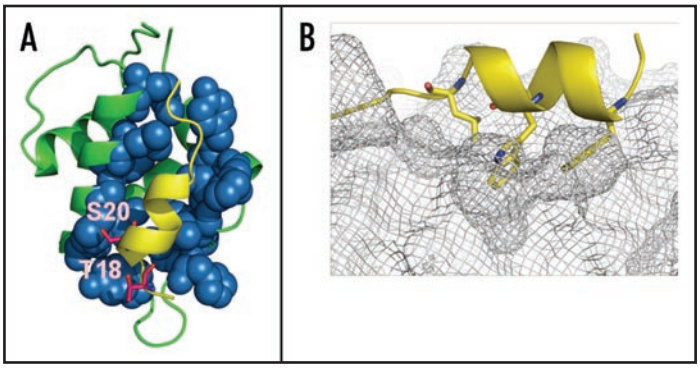

Figure 1. Structure of the p53-MDM2 complex taken from the crystal structure 1YCR[14] (A) Ribbon representation of MDM2 and p53 peptide in green and yellow respectively. MDM2 residues that interact with p53 are shown as blue spheres. The sites of phosphorylation on p53 i.e., Ser15, Thr18 and Ser20 are shown as sticks (B) Close-up of the p53 peptide (in yellow), with three critical residues, F19, W23, L26, shown in sticks, buried deeply in the MDM2 core (represented in grey wire mesh).

sites were found to be extensively phosphorylated in a panel of human breast cancers.[29] CK1 (casein kinase 1;[22,27] and Chk2[23] are known to phosphorylate Thr18 and Ser20 respectively. Overexpression of Vrk1 (Vaccinia-related kinase 1) has been shown to increase endogenous p53 phosphorylation at Thr18.[30] Synthetic-peptide binding assays have demonstrated unequivocally that phosphorylation of either Thr18 or Ser20 leads to diminished MDM2 binding.[29,31] The structural data show that these two residues are not involved in any direct contacts with MDM2; however, in p53, the sidechains of Thr18 and Asp21 are involved in an hbond (yellow peptide in Fig. S2). This has lead to speculations that this interaction is important for the initiation of formation of the p53TAD helix which is needed for optimal binding to the MDM2 cleft.[14] Phosphorylation of the Thr18 sidechain would introduce a negative charge that would lead to repulsions with the anionic Asp21, loss of the hbond and loss of helicity of the peptide. This would explain the loss of interaction between p53TAD and MDM2. In addition, the introduction of a large negative charge upon phosphorylation of the p53 peptide could be subject to electrostatic modulation by the electrostatic character of the MDM2 surface itself; although some experimental evidence suggests otherwise,[31] this subject has, to our knowledge, never been explored in detail. We now set out to dissect, through molecular dynamics (MD) simulations, the structural and energetic consequences of phosphorylation of Thr18 on the p53-MDM2 interactions. We also examine the implications for the p53-MDM4 interactions using a model we have constructed of the latter. Work in other laboratories has shown that protein dynamics and the effects of phosphorylations can reliably and successfully be explored using current computational methods.[32,33]

METHODS

The crystal structure of the human p53-MDM2 complex [Protein Data Bank code: 1YCR, resolved at 2.6 Å;[14] Fig. 1A] was used as the starting model for our studies. These included residues 25-109 of human MDM2 and residues 17–29 of human p53. The N- and C- termini of MDM2 were capped with acetyl (ACE) and N-methyl (NME) respectively to keep them neutral; the N-terminii of

p53 peptides were capped with ACE.[44] Systems were prepared in accordance with standard protocols ensuring appropriate conformational/protonation states using WHATIF.[54]

Molecular dynamics simulations were performed with the SANDER module of the AMBER8[55] package employing the all-atom Cornell force field.[56] Simulations were carried out for the complexes of p53-MDM2, the complexes of MDM2 and p53 phosphorylated at Thr18 and at Ser20 and doubly-phosphorylated (at Thr18 and Ser20). In addition, simulations were also carried out for the uncomplexed protein and peptides (both phosphorylated and unphosphorylated) separately. Simulations were also carried out for mutant MDM2 complexes. Each system was solvated in a cubic TIP3P water[57] box that extended at least 12 Å in each direction from the solute. Non-bonded van der Waals interactions were truncated at 10 Å. All bonds involving hydrogen atoms were constrained using SHAKE.[58] Particle mesh Ewald (PME)[59] was coupled with periodic boundary conditions. After initial minimizations, the systems were gradually heated to 300 K, equilibrated for 100 ps and finally subject to simulations of 10 ns (20 ns for the free peptides). In total we performed 14 simulations, totaling 180 ns.

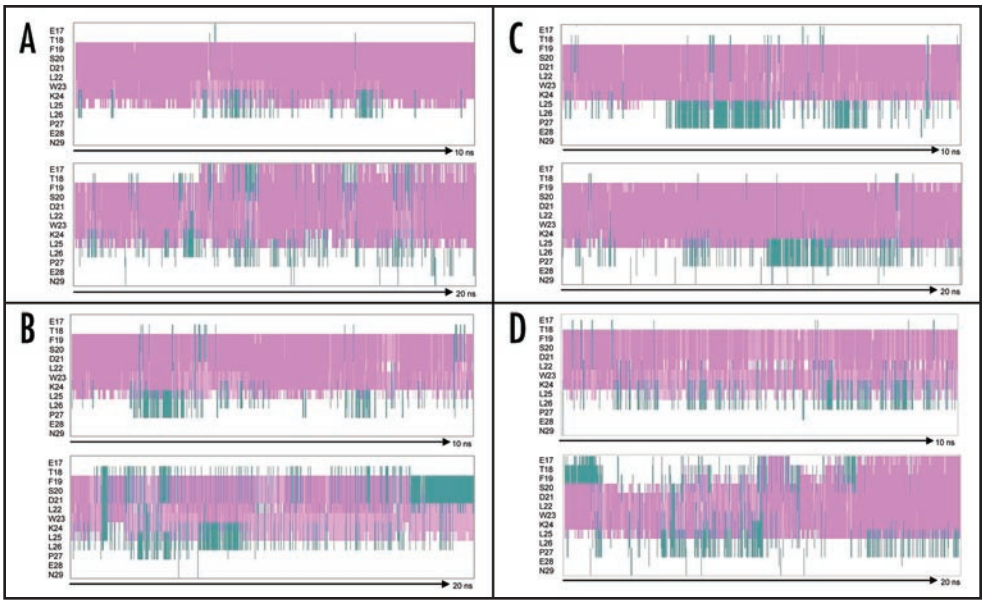

Figure 2. Temporal evolution of the secondary structure profiles p53 peptides over simulations of 10 ns (for the bound peptides) and 20 ns (for the free peptides). (A) WTp53 (B) p53pT18 (C) p53pS20 (D) p53pT18pS20. Each section consists of two profiles corresponding to bound (top) and free (bottom) peptide. The secondary structure is colored as follows: dark pink, α-helix; light pink, 3–10 helix; cyan, turn; while, random coil.

Free energy of binding (ΔG_{bind}) of the peptides to MDM2 was computed using the MM-GBSA (molecular mechanics/Generalized Born surface area) method[60,61] using the GB module[62] in Amber while the non-polar component is estimated from the solvent accessible surface area using MOLSURF[63] using: $\Delta G_{solv,np}$ = 0.00542*SASA + 0.92.[64] Each energy term was averaged over frames taken every 2 ps from the simulation. Vibrational entropy was estimated using normal mode analysis (Nmode module of Amber)[65] and averaged over 200 ps intervals. Electrostatic calculations were done using APBS.[47] Secondary structures were computed using STRIDE.[66] PyMOL[67] and Visual Molecular Dynamics (VMD) was used for visualizations.[68]

RESULTS AND DISCUSSION

The MD simulations are stable as judged by the temporal evolution of the Root Mean Square Deviation (RMSD) of the Cα atoms (Fig. S3A and B); higher variability is seen in the free peptides as expected. Fluctuations of the Cα atoms within MDM2 are similar in pattern to those seen in the crystal structure (Fig. S4A), differing mainly in regions that bind peptides. The extent of the changes upon phosphorylations is similar, suggesting that the peptides bind in a similar manner. Their fluctuations, as expected, are lower in the bound state (by two- to four-fold); amongst the free peptides, the peptide phosphorylated at Ser20 (pSer20) exhibits the lowest fluctuations (S4B).

Examination of the secondary structure evolution of the peptides (Fig. 2A–D) shows that the peptides exist as interconverting conformers; the helical conformation is dominant, in particular in the region that displays the sidechains of Phe19 and Trp23; the latter is essential for binding.[17] This is in agreement with NMR observations that the Thr18-Leu26 region is helical in solution.[34] Interestingly, the free peptides exist largely in helical conformations even upon phosphorylation; this feature is in contrast to the belief that the addition of a phosphate group would destabilize the helix.[14]

The crystal structure shows the following hbonds between the wild type p53 (WTp53) peptide and MDM2 (Fig. S2): between Glu17 and MDM2-Lys94 sidechains, Asp21 and Thr18 sidechains and backbones, Trp23 sidechain and MDM2-Leu54 backbone, Asn29 and MDM2-Glu25 sidechains and between the C-terminal carboxylate and MDM2-Tyr100/Tyr104 sidechains. The Ser20 sidechain is not involved in any local interactions, pointing towards MDM2-Met62 (separated by 3.1 Å). In the simulations of the WTp53-MDM2 complex, the hbonds that are retained are those between Trp23 and Leu54 and between the C-terminus and Tyr100. In addition, the C-terminus is also found to interact with Arg97. During the simulations of the free WTp53 peptide, the Thr18-Asp21 hbond exists for only 5% of the total time; however, Asp21 is stabilized by Lys24 (Fig. 3A) for about 2 ns. This salt bridge has been deemed as "helix-stabilizing" in NMR studies.[34] Upon phosphorylations of Thr18 (pThr18), Asp21 is still stabilized by Lys24 while the pThr18 now finds an alternate interaction with the Ser20 sidechain hydroxyl (Fig. 3B, stable > 60% of 20 ns); in addition it also forms an hbond (> 40% of 20 ns) with the Ser20 backbone. This is also seen in the pThr18-MDM2 simulation. Again in free pSer20, the phosphorylated Ser20 sidechain makes hbonds both with the Thr18 sidechain as well as with the Lys24 sidechain and backbone (Fig. 3C); Asp21 makes hbonds with the Glu17 backbone. In the case of the doubly phosphorylated p53 peptide (pThr18pSer20), the phosphate group of Ser20 makes a hbond with sidechain of Lys24 for more

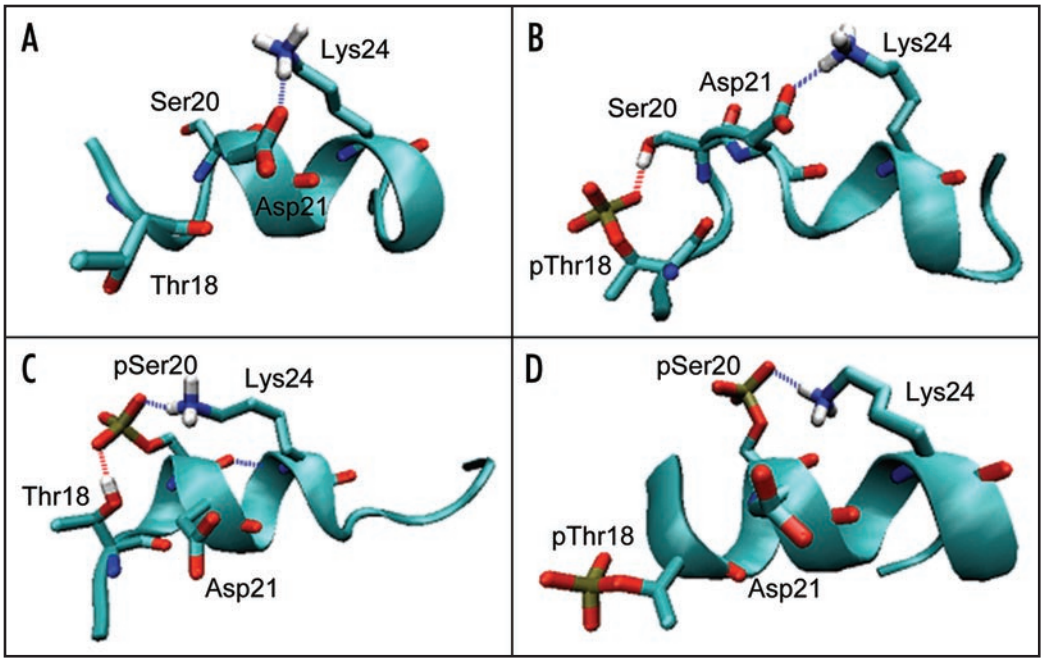

Figure 3. Helix-stabilizing hbonds observed during 20 ns simulation of the free p53 peptide (residues 17–29): (A) WTp53 (B) p53pT18 (C) p53pS20 (D) p53pT18pS20.

Table 1 **Binding free energy of MDM2 with WT/phosphorylated p53 peptide**

System	Enthalpy	Entropy	ΔG
p53	-44.66	-37.77	-6.89
p53pT18	-36.52	-34.40	-2.12
p53pS20	-44.88	-40.47	-4.41
p53pT18pS20	-36.24	-42.41	+6.17

*Values are in kcal/mol

than 50% of 20 ns, while the phosphate group of Thr18, originally found to interact with Ser20, is now fully solvated (Fig. 3D). The remaining sidechains are either completely solvated or are bridged by intervening water molecules. Thus, even though Asp21 and phosphorylated Thr18 repel each other, there is enough flexibility in the peptide and there are enough potential hbonding options for these sidechains to make alternate/new hbonds, without causing the helix to unfold. The role of Asp21 in helping maintain the helix may not be as critical since mutation to Ala does little by way of affecting the interactions of this peptide with MDM2.[17,35] The mouse sequence (Fig. S1B) has a Gly in place of Asp21. Lys24 seems to be important in forming helix-stabilizing hbonds in unphosphorylated and phosphorylated states; this residue is Lys only in human and mouse but is replaced by Ser or Asn, both of which have potentials to form hbonds through their sidechains. The tight binding peptide 12-1[36] has a Glu in this position, which although opposite in polarity, will still hbond with the Thr18 sidechain, although the Thr has now been replaced by Arg. The frog sequence contains Glu in place of Ser20; perhaps this acts as a phosphomimic, so the binding characteristics of pThr18 (Thr17 in frog) will be similar to those of doubly phosphorylated human p53 peptide. Overall, the larger number of hbonds that exist as a result of phosphorylations lead to lower fluctuations (Fig. S4B). This is particularly evident in the reduced fluctuations in Thr18, Ser20, Asp21 and Lys24, all of which are involved in hbonds that help maintain the helical conformations. The reduction in Trp23 arises from the formation of hbonds between the backbone atoms of Trp23 and Lys24. Together we see that the phosphorylated states have several altered interactions, all of which help to stabilize the helical conformations through increased hbonding. Other simulation studies have reported such increases in the helicity of peptides.[37,38]

In summary, our simulations suggest that all the peptides are equally likely to be helical in their free states to different extents and bind to MDM2 in an apparently similar manner; this stems from the persistent helicity of the Phe19-Trp23 region which is a requisite for optimal binding to MDM2. Our findings are corroborated by NMR studies showing that regions of p53TAD are helical, particularly between Thr18 and Leu26.[34,39]

Energetics of phosphorylation. Binding affinities are currently computed reliably using continuum methods.[40-42] For the complexation of a ligand (peptide) and a receptor protein, the free energy of binding (ΔG_{bind}) is computed either by calculating the average values of G separately for the ligand, receptor and complex from a single MD simulation of the complex (Method 1) or by extracting values from simulations that are run separately on the complex, ligand and receptor (Method 2). Kollman[43] computed ΔG_{bind} of a human p53 peptide (residues 16-27) with *X. laevis* MDM2 as -4.52 (Method1) and -2.39 kcal/mol (Method 2), close to the experimental data (-6.6 to -7.8 kcal/mol). Carlson[44] obtained values (-7.4 kcal/mol) of the human p53-MDM2 complex that were even closer, using a combination of the two methods.

The experimentally reported value[36] of IC_{50} for the binding of the p53 peptide (residues 16-27) to MDM2 was 2-14 μM (ΔG_{bind} of ~-6.6 to -7.8 kcal/mol). This value is similar to that reported for peptides corresponding to the region 15-29.[31] We use the 17-29 region as this had defined density in the crystallographic structure.[14] The ΔG_{bind} from our simulations based on Method 2, is -6.9 kcal/mol (Table 1 and S1A), in very good agreement with experiments[31,36] (we get ΔG_{bind} of -19.6 kcal/mol and -3.1 kcal/mol using Method 1 and the combination respectively). The computed values of enthalpy and entropy are similar to those reported by Kollman[43] and Carlson.[44] Although our overall ΔG_{bind} values are close to the experimental ones, the magnitudes of the components are large;[31] of course the temperature of the experiments was only 15°C and it is not clear what the effects of increased temperature would be. It is clear from (Table S1A) that the enthalpy computed from a single trajectory is overestimated because the transient non-optimal states that are

sampled in trajectories of the free peptides (as seen for example in the larger variability in the RMSD of Fig. S3A) are not sampled. For the rest of this study, only results obtained using Method 2, which seems to reflect the actual process, will be discussed (detailed results are in Table S1). In contrast to ΔG_{bind} of -6.9 kcal/mol for the WTp53, we compute -2.1 kcal/mol, -4.4 kcal/mol and +6.2 kcal/mol for pThr18, pSer20 and pThr18pSer20 respectively (Table 1). These consist of enthalpies of -44.7 kcal/mol, -36.5 kcal/mol, -44.9 kcal/mol and -36.2 kcal/mol for WTp53, pThr18, pSer20 and pThr18pSer20 respectively. WTp53 pays a larger desolvation penalty (+32 kcal/mol) compared to pThr18 (+27 kcal/mol). This arises because the conformation of free pThr18 is more compact from the extra hbonds that phosphorylation creates, thereby incurring less desolvation costs. However, this is compensated by more favorable intramolecular vdWs interactions (-70 kcal/mol vs. -66 kcal/mol) and lower internal energy (+1.6 kcal/mol vs. +9.7 kcal/mol), resulting in a more favorable ΔG_{bind} of the WTp53 peptide. The desolvation penalty for pSer20 is lowest (+20 kcal/mol), with intramolecular vdWs of -61 kcal/mol and internal energy of +4.9 kcal/mol, which leads to an overall enthalpy that is similar to WTp53, but more favorable than that of pThr18. However, due to a somewhat larger entropic loss in pSer20 (~3 kcal/mol), WTp53 yields a more favorable ΔG_{bind} than pSer20. In contrast, a high desolvation (+36 kcal/mol) and entropic penalty (+42.5 kcal/mol) suggests that pThr18pSer20 will not bind to MDM2.

Fersht's group[31] have estimated ΔG_{bind} of the WTp53, pThr18, pSer20 and pThr18pSer20 peptides, to be -8.2, -7.3, -8.5 and -7.3 kcal/mol respectively. Our results do show a similar trend. The enthalpies of WTp53 and pSer20 are similar to each other while that of pThr18 and pThr18-pSer20 are reduced. The higher enthalpy of pThr18 relative to the wild type and pSer20 is in agreement with the much higher k_{off} values observed for pT18[31] and with observations that pThr18 attenuates the binding affinity of p53 to MDM2 more than pSer20 does.[29] The contrast is in the case of the doubly phosphorylated system which should not bind and yet the experimental observations suggest otherwise.[31] The experiments were carried out at a temperature 22°C lower than the simulations and it is possible that the higher entropy that is characteristic at higher temperatures (Table S1) leads to a larger penalty upon binding, leading to the computed unfavorable ΔG_{bind}.

Contributions of individual residues. Figure S5 show the contributions from individual residues to the p53-MDM2 interactions. It is encouraging to note that the three critical residues of p53 (Phe19, Trp23 and Leu26) contribute the most. Thirteen of the 14 MDM2 residues that are involved in making contacts with the peptide in the crystal and identified in NMR[45] also contribute significantly; in addition, Lys51, Gln72, and Arg97 contribute >1 kcal/mol, interacting favorably with Glu28, Thr18 and the p53 C-terminus respectively. On the other hand, Ser20 and Lys24 of p53 are destabilizing. This is in agreement with Kollman's alanine scanning mutagenesis[43] and separately, a high affinity peptide contains Met20.[36] Lys24, is exposed and does not make any interactions with MDM2; the optimized peptide pulled down by Lane and coworkers[36] shows this Lys to be replaced by Glu (Fig. S6); however, there seems to be a correlated mutation in position 18 leading to a cationic change from Thr to Arg.

The introduction of a phosphate group at either Thr18 or Ser20 destabilizes the interactions of pThr18 (+2.04 kcal/mol; -1.00 kcal/mol in the WT) and of pSer20 (+2.91 kcal/mol; +0.7 kcal/mol in the WT). In MDM2, significant destabilization is incurred only for Asp68 (+0.63 kcal/mol from +0.29 kcal/mol) and Glu69 (+0.64 kcal/mol from +0.39 kcal/mol). However, all anionic residues (D46, E52, D68, E69, D80, D84, E95), located as far away as 26 Å, undergo destabilization, albeit by a small amount <0.5 *kT*); long range perturbations have been reported in NMR studies.[45] Similarly, the introduction of the negative charges (phosphates) stabilize the cationic residues, mostly by up to ~*kT*; exceptions are Lys51 and Arg97, located ~16 and 25 Å from the sites of phosphorylation, which are stabilized by 2.5–3 *kT*. Lys94, located ~11 Å from Thr18 is stabilized significantly only upon double phosphorylation; interestingly, Arg97 is one of the three residues that differ between MDM2 and MDM4 (Ser in this p53TAD binding domain.[18] This again reflects both the long range and the complex nature of conformational modifications that take place as a result of peptide binding in MDM2.[45] Indeed, when the peptide is doubly phosphorylated, the interactions of pThr18 and pSer20 are destabilized relative to that in the wild type (+0.45 and +2.66 kcal/mol respectively).

Electrostatics of MDM2. Together, the experimental data of Fersht and coworkers[31] and our computed binding free energies suggest that phosphorylated p53 peptides do bind to MDM2, albeit with a reduced affinity. And yet we know that upon phosphorylation, the binding of p53 to MDM2 is abrogated. We assume that the peptides used in these studies mimic, at least qualitatively, the binding of full length p53TAD. We find that helicity of p53 is not disrupted upon phosphorylation. This suggests that there must be some additional characteristic that contributes to this abrogation. So we decided to examine features of the MDM2 surface (electrostatics) that an oncoming peptide/protein would "see" from a long range.[46] Studies by Fersht and coworkers have found no evidence of any surface charge effects on this binding. Our own computations, in agreement with these observations, also show a small (2–3 kcal/mol) destabilization of binding energies as the salt concentration is raised even as much as two-fold (data not shown). However our computations also show that, of the net interaction energies for complexation, with MDM2 contributing -33 to -38 kcal/mol and p53 in its various states ranges contributing -21 to -27 kcal/mol, at least 25% in MDM2 arises from the charged residues while in p53, the major component arises from the phosphorylated residues. This amounts to ~6–8 kcal/mol arising from electrostatics and clearly reflects that the overall interaction is modulated by electrostatics to some extent. We decided to examine this more qualitatively through computations of the potentials in the Poisson-Boltzmann approximation.[47]

The N-terminal domain of MDM2 has a net charge of +5; this is evident from the large blue cover that engulfs the protein surface (Fig. 4A). At first glance, this suggests enhanced binding of p53 peptides that have an additional anionic charge as a consequence of phosphorylation. This seems contrary to the abrogation of binding. We notice regions of anionic patches (in red) and in particular we see that the sidechains of Thr18 and Ser20 of WTp53 are located in the vicinity of such localized anionicity. It is clear why phosphorylated Ser15 does little by way of interrupting the p53-MDM2 interaction,[26,27] as the phosphoryl group sits in a cationic region (Fig. S7). Thr18 sits near an anionic region while Ser20 is localized on its edges. This suggests that upon phosphorylations, these peptides will experience charge-charge repulsions from these regions on the MDM2 surface. For optimal binding, since a helical conformation

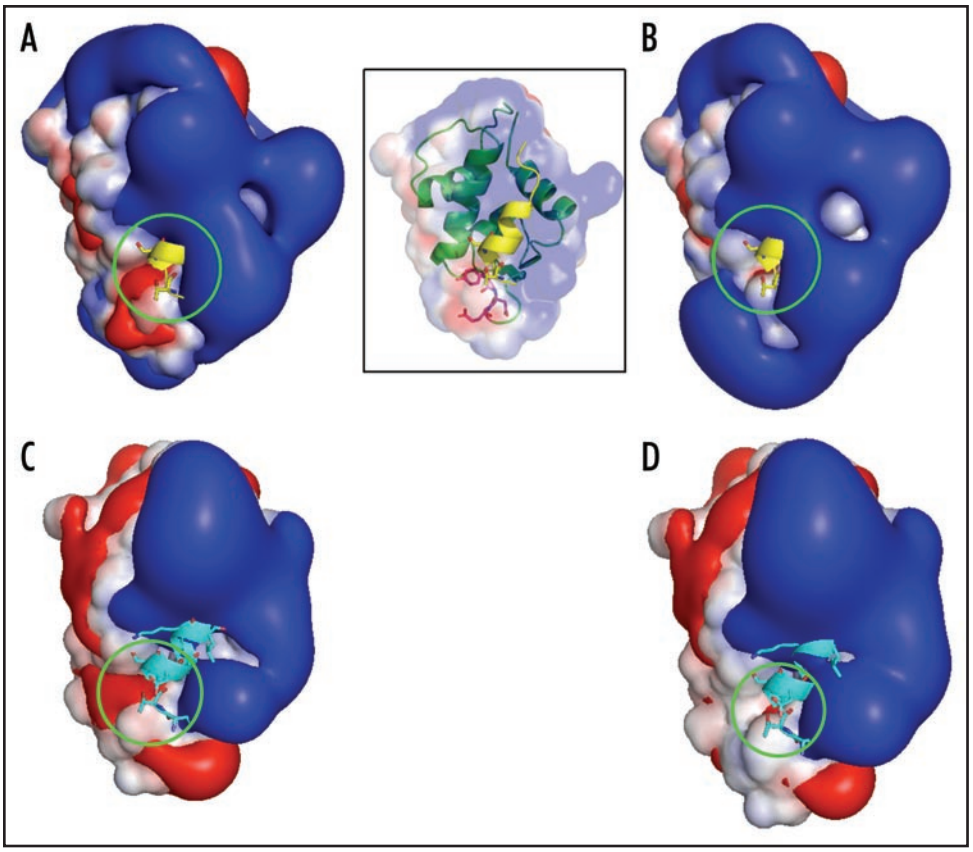

Figure 4. Electrostatic potential mapped on to the solvent accessible surface of (A) MDM2 and (B) MDM2 triple mutant, Y67F, D68N, E69Q (C) MDM2 and (D) MDM4 double mutant Y44F, D45N. Positions of Y67, D68 and E69, drawn in red sticks, are shown in inset. The potentials are color coded from blue (+1 kcal e^{-1} mol^{-1}) to red (-1 kcal e^{-1} mol^{-1}). The p53 peptide is shown in yellow ribbon representation, and residues Thr18 and Ser20 are drawn in sticks (in green circle).

Table 2 **Binding free energy of MDM2 triple mutant with WT/phosphorylated p53 peptide**

System	Enthalpy	Entropy	ΔG
p53	-54.23	-44.37	-9.86
p53pT18	-54.05	-34.51	-19.54
p53pS20	-45.59	-42.13	-3.46/-18.24#
p53pT18pS20	-52.02	-45.93	-6.09

*Values are in kcal/mol. #Binding free energy of p53pS20 to MDM2 quadruple mutant

of the peptide is required, this implies that the two phosphorylated sidechains will be constrained to remain in conformations that cannot be too different from those seen in the unphosphorylated bound state. In order to test this, mutations of these sites into residues of opposite polarities should mitigate this interaction and enhance the binding of the phosphorylated peptides. Indeed, if one were to examine the structure of the optimized p53 peptide (MPRFMDYWEGLN), that bound 35-fold tighter compared to WTp53 peptide,[18,36,48] we see that Thr18 is replaced with cationic Arg (Fig. S6); Ser20 is replaced by Met; Lys24 sidechain which "floats" in a cationic region is replaced by Glu. In order to test our hypothesis, we constructed a triple mutant: Tyr67Phe, Asp68Asn and Glu69Gln, to abolish the anionic patch on MDM2; the change to enhanced cationicity is evident from the replacement of the red in Figure 4A to blue in Figure 4B; when such surface residues are mutated, perturbation to the overall structure is minimal;[49] the secondary structure of mutant MDM2 remains unperturbed during the simulations (Fig. S8).

Affinity of p53 for the MDM2 triple mutant. The computed ΔG_{bind} of both WTp53 and pThr18 to the triple mutant-MDM2 (Table 2 and S2) was significantly enhanced (WTp53 increases ~2.5 kcal/mol and pThr18 increases by ~17 kcal/mol, with the major contribution arising from the enthalpic component). While pThr18 undergoes an almost ten-fold increase in binding affinity, surprisingly, pSer20 is destabilized by ~1 kcal/mol. Interestingly, the doubly phosphorylated peptide now has a negative ΔG_{bind} (-6.1 kcal/mol). This suggests that phosphorylation of Thr18 is the major regulator of the interaction of p53 with MDM2. Indeed the introduction of phosphorylation at Ser20 does bring down the ΔG_{bind} from -19 kcal/mol for pThr18 to -6 kcal/mol. The fact that the doubly phosphorylated p53 will not bind at all to MDM2 is suggestive of levels of control perhaps of the p53 activity. We note that phosphorylation of Ser20 localizes the phosphate moiety to the vicinity of the negatively charged sulphur of Met62, which causes charge-charge repulsions (Fig. S9A). The optimized peptide 12/1 consists of a Met in place of Ser20 (Fig. S6).[36] We mutated the triple mutant further, with Met62 replaced by Lys (Fig. S9B; Table 2) and found that the binding of pSer20 increases from -3.5 to -18 kcal/mol. These repulsions are reflected in the shift that the peptides undergo during the simulations. We started the simulations with the docked pose adopted by WTp53 as observed in the crystal structure. In Figure S10A–C we see how the wild type pose of the peptide remains, while for all the phosphorylated systems, the repulsions "push" the peptides away from their original axial direction by ~20–30° (the top views) and also force them "off" the surface (as viewed by the clear displacements of the Phe19 and Trp23 rings away from MDM2 in the views on the right); the triple mutant (Fig. S10D) shows that both WTp53 and pThr18 bind "snugly" (animations of these movements can also be seen in www.bii.a-star.edu.sg/~chandra/HJ-cellcyclep53phos.html). What may the relevance be of such mutations in a biological context? MDM2 splice variants are known to be important in cancer cell lines.[50] While most known splice variants of MDM2 have the p53TAD binding region of MDM2 missing, there are variants with parts of this region intact, such as the Δ1–49 variant.[51] It remains to be seen if other MDM2 splice variants or mutations exist in cancer cells that may not only bind p53 but also the phosphorylated forms of p53, thereby exerting additional downregulation of tumor suppression by p53.

Affinity of p53 for MDM4. MDM4 is a structural homologue of MDM2 and is known to inhibit p53 activity.[11,52,53] While the detailed mechanism of regulation of p53, MDM2 and MDM4 is complex, the N-terminal region of MDM4 is known to modulate the levels of p53 too. A recent structural study of the N-terminal domain of MDM4 complexed with the transactivation region of p53[19] has identified some structural differences, mainly in the orientation of residues in one part of the p53-binding cleft, which may underlie the differential interactions between p53 and MDM4 (compared to p53 and MDM2).[18] Electrostatic maps of MDM4 (Fig. 4C) show, in a manner similar to MDM2, that the phosphorylated-Thr18 of p53 will lie in the vicinity of an anionic patch on the surface of MDM4 and experience repulsion. The affinity of the optimized p53 peptide, with Arg in place of Thr18 and Glu in place of Lys24 binds tighter to MDM4 than does wild type p53, as it does for MDM2.[18] This suggests that the local electrostatics do modulate the binding in MDM4 also, similar to that seen for MDM2. We constructed a double mutant (the residues corresponding to Y67-D68-E69 of MDM2 are Y44-D45-Q46 in MDM4) and we see that, as seen in MDM2, the potential in MDM4 is indeed attenuated (Fig. 4D) and this mutant should show enhanced binding of the p53-peptide phosphorylated at Thr18. Simple binding energy calculations (data not shown) again show the same pattern of energetics as is seen for MDM2, although the affinity of the peptides for MDM4 is lower than for MDM2; this is in agreement with experimental observations.[18] A direct comparison with the "humanized" structure of zebrafish MDM4 is not possible because there are key differences in the residues that lie in the region that binds Nterminal end of the p53 peptide. For example, a salt bridge between Arg65 and Glu69 in MDM2 is not present in this humanized form (residues are replaced by Gln61 and Lys65 respectively). Salt bridges will no doubt influence the local electrostatics and hence the modulation of the binding of phosphorylated peptides. We keenly await the crystal structure of human MDM4 (and associated binding experiments with phosphorylated peptides) to see if the mutations suggested in this study do enable the binding of phosphorylated p53 to MDM2/MDM4 and present a new insight into regulation of this complex p53-MDM2-MDM4 pathway.

CONCLUSION

Molecular dynamics simulations and electrostatic analyses of the interaction between peptides from the transactivation domain of p53 and the N-terminal region of MDM2 have been carried out to understand how the phosphorylation of p53 transactivation domain residues Thr18 (and Ser20) modulates its binding to MDM2 (and MDM4), thus upregulating p53 levels in stressed cells. We find that the p53 peptides are stable as helical conformations in solution, irrespective of their phosphorylation status. This is in contrast to the widely held belief that phosphorylation of Thr18 disrupts a stable helix-promoting interaction (this helix is necessary for optimal binding of p53 to MDM2) between the sidechains of Thr18 and Asp21. We find instead that a hitherto overlooked feature, that of local anionicity, in the electrostatic features of the MDM2 (and MDM4) surface seems responsible for abrogating interactions with the phosphorylated p53 through a charge-charge repulsion between anionic regions of MDM2 and the negatively charged phosphate moiety on p53TAD that develops as a response to stress-related signaling. The findings are backed by detailed energetic calculations and electrostatic analyses. The latter establish a physical basis for the high affinity p53TAD-like peptide that has been identified. A triple and a quadruple mutant have been constructed for MDM2 (a double mutant for MDM4) that remove this anionicity from the MDM2 (and MDM4) surface and leads to enhanced binding of pThr18, pSer20 and pThr18-pSer20.

This may have implications for an additional level of control in the complex interplay between p53, MDM2 and MDM4. On the one hand it may offer a novel handle on the design of therapeutics against MDM2/MDM4 to stabilize wild type p53 and on the other it may shed light on the role of potential splice variants and mutants/SNP of MDM2/MDM4 as they are being unraveled.

References

1. Hollstein M, Sidransky D, Vogelstein B, Harris CC. p53 mutations in human cancers. Science 1991; 253:49-53.
2. Harris CC. p53 Tumor suppressor gene: From the basic research laboratory to the clinic - An abridged historical perspective. Carcinogenesis 1996; 17:1187-98.
3. El-Deiry W. Regulation of p53 downstream genes. Semin Cancer Biol 1998; 8:345-57.
4. Webster GA, Perkins ND. Transcriptional cross talk between NF-kappaB and p53. Mol Cell Biol 1999; 19:3485-95.
5. Raman V, Martensen SA, Reisman D, Evron E, Odenwald WF, Jaffee E, Marks J, Sukumar S. Compromised *HOXA5* function can limit p53 expression in human breast tumors. Nature 2000; 405:974-8.
6. Woods DB, Vousden KH. Regulation of p53 Function. Exp Cell Res 2001; 264:56-66.
7. Momand J, Wu HH, Dasgupta G. MDM2 - Master regulator of the p53 tumor suppressor protein. Genes 2000; 242:15-29.
8. Barak Y, Juven T, Haffner R, Oren M. Mdm2 expression is induced by wild type p53 activity. EMBO J 1993; 12:461-8.
9. Wu X, Bayle JH, Olson D, Levine AJ. The p53-mdm-2 autoregulatory feedback loop. Genes Dev 1993; 7:1126-36.
10. Shvarts A, Steegenga WT, Riteco N, van Laar T, Dekker P, Bazuine M, van Ham RC, van der Houven van Oordt W, Hateboer G, van der Eb AJ, Jochemsen AG. MDMX: A novel p53-binding protein with some functional properties of MDM2. EMBO J 1996; 15:5349-57.
11. Marine J, Jochemsen AG. Mdmx and Mdm2: Brothers in arms? Cell Cycle 2004; 3:900-4.
12. Stommel J, Wahl GM. A new twist in the feedback loop: Stress-activated MDM2 destabilization is required for p53 activation. Cell Cycle 2005; 4:411-7.
13. Ghosh M, Weghorst K, Berberich SJ. Mdmx inhibits ARF mediated Mdm2 sumoylation. Cell Cycle 2005; 4:604-8.
14. Kussie PH, Gorina S, Marechal V, Elenbaas B, Moreau J, Levine AJ, Pavletich NP. Structure of the MDM2 oncoprotein bound to the p53 tumor supressor transactivation domain. Science 1996; 274:948-53.
15. Yu GW, Rudiger S, Veprintsev D, Freund S, Fernandez-Fernandez MR, Fersht AR. The central domain of HDM2 provides a second binding site for p53. Proc Natl Acad Sci USA 2006; 103:1227-32.
16. Lin J, Chen J, Elenbaas B, Levine AJ. Several hydrophobic amino acids in the p53 amino-terminal domain are required for transcriptional activation, binding to mdm2 and the adenovirus 5 E1B 55-kD protein. Genes Dev 1994; 8:1235-46.
17. Uesugi M, Verdine GL. The alpha-helical FXXPhi Phi motif in p53: TAF interaction and discrimination by MDM2. Proc Natl Acad Sci USA 1999; 96:14801-6.
18. Bottger V, Bottger A, Garcia-Echeverria C, Ramos YF, van der Eb AJ, Jochemsen AG, Lane DP. Comparative study of the p53-mdm2 and p53-MDMX interfaces. Oncogene 1999; 18:189-99.
19. Popowicz G, Czarna A, Rothweiler U, Szwagierczak A, Krajewski M, Holak T. Molecular basis for the inhibition of p53 by Mdmx. Cell Cycle 2007; 6, (In press).
20. Lees-Miller SP, Sakaguchi K, Ullrich SJ, Appella E, Anderson CW. Human DNA-activated protein kinase phosphorylates serines 15 and 37 in the amino-terminal transactivation domain of human p53. Mol Cell Biol 1990; 12:5041-9.
21. Abraham RT. Cell cycle checkpoint signalling through the ATM and ATR kinases. Genes Dev 2001; 15:2177-96.
22. Dumaz N, Milne DM, Meek DW. Protein kinase CK1 is a p53-threonine 18 kinase which requires prior phosphorylation of serine 15. FEBS Lett 1999; 463:312-6.
23. Hirao A, Kong YY, Matsuoka S, Wakeham A, Ruland J, Yoshida HD, Elledge SJ, Mak TW. DNA damage-inducible activation of p53 by the checkpoint kinase Chk2. Science 2000; 287:1824-7.
24. Shieh SY, Ahn J, Tamai K, Taya Y, Prives C. The human homologs of checkpoint kinases Chk1 and Cds1 (Chk2) phosphorylate p53 at multiple DNA damage-inducible sites. Genes Dev 2000; 14:289-300.
25. Helt CE, Cliby WA, Keng PC, Bambara RA, O'Reilly MA. Ataxia telangiectasia mutated (ATM) and ATM and RAD3-related protein exhibit selective target specificities in response to different forms of DNA damage. J Biol Chem 2005; 280:1186-92.

26. Meek DW, Campbell LE, Jardine LJ, Knippschild U, McKendrick L, Milne DM. Multi-site phosphorylation of p53 by protein kinases inducible by p53 and DNA damage. Biochem Soc Trans 1997; 25:416-9.
27. Sakaguchi K, Saito S, Higashimoto Y, Roy S, Anderson CW, Appella E. Damage-mediated phosphorylation of human p53 threonine 18 through a cascade mediated by a casein 1-like kinase: Effect on Mdm2 binding. J Biol Chem 2000; 275:9278-83.
28. Dumaz N, Milne DM, Jardine LJ, Meek DW. Critical roles for the serine 20, but not the serine 15, phosphorylation site and for the polyproline domain in regulating p53 turnover. Biochem J 1999; 359:459-64.
29. Craig AL, Burch L, Vojtesek B, Mikutowska J, Thompson A, Hupp TR. Novel phosphorylation sites of human tumor suppressor protein p53 at Ser20 and Thr18 that disrupt the binding of mdm2 (mouse double minute 2) protein are modified in human cancers. Biochem J 1999; 342:133-41.
30. Vega FM, Sevilla A, Lazo PA. p53 Stabilization and accumulation induced by human vaccinia-related kinase 1. Mol Cell Biol 2004; 24:10366-80.
31. Schon O, Friedler A, Bycroft M, Freund SMV, Fersht AR. Molecular mechanism of the interaction between MDM2 and p53. J Mol Biol 2002; 323:491-501.
32. Young MA, Gonfloni S, Superti-Furga G, Roux B, Kuriyan J. Dynamic coupling between the SH2 and SH3 domains of c-Src and Hck underlies their inactivation by C-Terminal Tyrosine phosphorylation. Cell 2001; 105:115-26.
33. Groban ES, Narayanan A, Jacobson MP. Conformational changes in protein loops and helices induced by post-translational phosphorylation. PLOS Comp Biol 2006; 2:238-50.
34. Lee H, Mok KH, Muhandiram R, Park KH, Suk JE, Kim DH, Chang J, Sung YC, Choi KY, Han KH. Local structural elements in the mostly unstructured transcriptional activation domain of human p53. J Biol Chem 2000; 275:29426-32.
35. Zondlo SC, Lee AE, Zondlo NJ. Determinants of specificity of MDM2 for the activation domains of p53 and p65: Proline27 disrupts the MDM2-binding motif of p53. Biochemistry 2006; 45:11945-57.
36. Bottger A, Bottger V, Garcia-Echeverria C, Chene P, Hochkeppel H, Sampson W, Ang K, Howard SF, Picksley SM, Lane DP. Molecular characterization of the HDM2-p53 interaction. J Mol Biol 1997; 269:744-56.
37. Shen TY, Wong CF, McCammon JA. Atomistic brownian dynamics simulation of peptide phosphorylation. J Am Chem Soc 2001; 123:9107-11.
38. Shen TY, Zong C, Hamelberg D, McCammon JA, Wolynes PG. The folding energy landscape and phosphorylation: Modeling the conformational switch of the NFAT regulatory domain. FASEB J 2005; 19:1389-95.
39. Rosal R, Pincus MR, Brandt-Rauf PW, Fine RL, Michl J, Wang H. NMR solution structure of a peptide from the mdm-2 binding domain of the p53 protein that is selectively cytotoxic to cancer cells. Biochemistry 2004; 43:1854-61.
40. Kollman PA, Massova I, Reyes C, Kuhn B, Huo S, Chong L, Lee M, Lee T, Duan Y, Wang Y, Donini O, Cieplak P, Srinivasan J, Case DA, Cheatham TE. Calculating structures and free energies of complex molecules: Combining molecular mechanics and continuum models. Acc Chem Res 2000; 33:889-97.
41. Still WC, Tempczyk A, Hawley RC, Hendrickson T. Semianalytical treatment of solvation for molecular mechanics and dynamics. J Am Chem Soc 1990; 112:6127-9.
42. Reyes CM, Kollman PA. Structure and thermodynamics of RNA-protein binding: Using molecular dynamics and free energy analyses to calculate the free energies of binding and conformational change. J Mol Biol 2000; 297:1145-58.
43. Massova I, Kollman PA. Computational alanine scanning to probe protein-protein interactions: A novel approach to evaluate binding free energies. J Am Chem Soc 1999; 121:8133-43.
44. Zhong H, Carlson HA. Computational studies and peptidomimetic design for the human p53-MDM2 complex. Proteins 2005; 58:222-34.
45. Schon O, Friedler A, Freund S, Fersht AR. Binding of p53-derived ligands to MDM2 induces a variety of long range conformational changes. J Mol Biol 2004; 336:197-202.
46. Janin J. The kinetics of protein-protein recognition. PROTEINS 1997; 28:153-61.
47. Baker NA, Sept D, Joseph S, Holst MJ, McCammon JA. Electrostatics of nanosystems: Application to microtubules and the ribosome. Proc Natl Acad Sci USA 2001; 98:10037-41.
48. Grasberger BL, Lu T, Schubert C, Parks DJ, Carver TE, Koblish HK, Cummings MD, LaFrance LV, Milkiewicx KL, Calvo RR, Maguire D, Lattanze J, Franks CF, Zhao S, Ramachandren K, Bylebyl GR, Zhang M, Manthey CL, Petrella EC, Pantoliano MW, Deckman IC, Spurlino JC, Maroney AC, Tomczuk BE, Molloy CJ, Bone RF. Discovery and cocrystal structure of benzodiazepinedione HDM2 antagonists that activate p53 in cells. J Med Chem 2005; 48:909-12.
49. Selzer T, Albeck S, Schreiber G. Rational design of faster associating and tighter binding protein complexes. Nature Struct Biol 2000; 7:537-41.
50. Chandler DS, Singh RK, Caldwell LC, Bitler JL, Lozano G. Genotoxic stress induces coordinately regulated alternative splicing of the p53 modulators MDM2 and MDM4. Can Res 2006; 66.
51. Haines DS, Landers JE, Engle LJ, George DL. Physical and functional interaction between wild-type p53 and mdm2 proteins. Mol Cell Biol 1994; 14:1171-8.
52. Francoz S, Froment P, Bogaerts S, De Clercg S, Maetens M, Doumont G, Bellefroid E, Marine J. Mdm4 and Mdm2 coorperate to inhibit p53 activity in proliferating and quiescent cells in vivo. Proc Natl Acad Sci USA 2006; 103:3232-7.
53. Laurie N, Donovan S, Shih C, Zhang J, Mills N, Fuller C, Teunisse A, Lam S, Ramos Y, Mohan A, Johnson D, Wilson M, Rodriguez-Galindo C, Quarto M, Francoz S, Mendrysa S, Guy R, Marine J, Jochemsen AG, Dyer M. Inactivation of the p53 pathway in retinoblastoma. Nature 2006; 444:61-6.
54. Vriend G. WHAT IF: A molecular modeling and drug design program. J Mol Graph 1990; 8:52-6.
55. Case DA, Darden TA, Cheatham TE, Simmerling CL, Wang J, Duke RE, Luo R, Merz KM, Wang B, Pearlman DA, Crowley M, Brozell S, Tsui V, Gohlke H, Mongan J, Hornak V, Cui G, Beroza P, Schafmeister C, Caldwell JW, Ross WS, Kollman PA. AMBER8. San Francisco: University of California, 2004.
56. Cornell WD, Cieplak P, Bayly CI, Gould IR, Merz KM, Ferguson DM, Spellmeyer DC, Fox T, Caldwell JW, Kollman PA. A second generation force field for the simulation of proteins, nucleic acids, and organic molecules. J Am Chem Soc 1995; 117:5179-97.
57. Jorgensen WL, Chandrasekhar J, Madura JD, Impey RW, Klein ML. Comparison of simple potential functions for simulating liquid water. J Chem Phys 1983; 79:926-35.
58. van Gunsteren WF, Berendsen HJC. Algorithms for macromolecular dynamics and constraint dynamics. Mol Phys 1977; 34:1311-27.
59. Darden T, York D, Pedersen L. Particle mesh Ewald: An N.log(N) method for Ewald sums in large systems. J Chem Phys 1993; 98:10089-92.
60. Bashford D, Case DA. Generalized Born models of macromolecular solvation effects. Annu Rev Phys Chem 2000; 51:129-52.
61. Tsui V, Case DA. Molecular dynamics simulations of nucleic acids with a Generalized Born solvation model. J Am Chem Soc 2000; 122:2489-98.
62. Jayaram B, Sprous D, Beveridge DL. Solvation free energy of biomacromolecules: Parameters for a modified Generalized Born model consistent with the AMBER force field. J Phys Chem B 1998; 102:9571-6.
63. Connolly ML. Solvent-accessible surfaces of proteins and nucleic acids. Science 1983; 221:709-13.
64. Sanner MF, Olson AJ, Spehner JC. Reduced surface: An efficient way to compute molecular surfaces. Biopolymers 1996; 38:305-20.
65. Case DA. Normal-mode analysis of protein dynamics. Curr Opin Struct Biol 1994; 4:285-90.
66. Frishman D, Argos P. Knowledge-based protein secondary structure assignment. Proteins 1995; 23:566-79.
67. DeLano WL. The PyMOL molecular graphics system. San Carlos, CA, USA: DeLano Scientific, 2002.
68. Humphrey W, Dalke A, Schulten K. VMD-visual molecular dynamics. J Mol Graph 1996; 14:33-8.